Natural Resources Canada | Ressources naturelles Canada

GEOLOGICAL SURVEY OF CANADA
OPEN FILE 8703

U-Pb zircon ages of plutonic rocks in the eastern Slave Craton and adjacent Thelon tectonic zone, Nunavut, determined by laser-ablation multi-collector inductively coupled mass spectrometry

R. G. Berman and A. Camacho

2020

Canada

GEOLOGICAL SURVEY OF CANADA
OPEN FILE 8703

U-Pb zircon ages of plutonic rocks in the eastern Slave Craton and adjacent Thelon tectonic zone, Nunavut, determined by laser-ablation inductively coupled multi-collector mass spectrometry

R. G. Berman[1] and A. Camacho[2]

[1]Geological Survey of Canada, 601 Booth Street, Ottawa, Ontario K1A 0E8
[2]University of Manitoba, 66 Chancellors Cir, Winnipeg, Manitoba R3T 2N2

2020

Permanent link: https://doi.org/10.4095/321633

This publication is available for free download through GEOSCAN (https://geoscan.nrcan.gc.ca/).

Recommended citation
Berman, R.G. and Camacho, A. 2020. U-Pb zircon ages of plutonic rocks in the eastern Slave Craton and adjacent Thelon tectonic zone, Nunavut, determined by laser-ablation inductively coupled multi-collector mass spectrometry; Geological Survey of Canada, Open File 8703, 1 .zip file. https://doi.org/10.4095/321633

Publications in this series have not been edited; they are released as submitted by the author.

CONTENTS

INTRODUCTION

The Thelon tectonic zone (Ttz) is a ~500 km long, northeast-striking geophysical and geological feature separating the Slave and Rae cratons of the Canadian shield (Fig. 1). The tectonic significance of the Ttz is uncertain, having been interpreted both as a Paleoproterozoic suture (Gibb and Thomas, 1977; Hoffman, 1988) and as an intracontinental orogenic belt (Thompson, 1989; Chacko et al., 2000; Schultz et al., 2007). Better understanding of the tectonic setting of the Ttz and the control of its crustal architecture on economic potential were primary goals of the Geomapping for Energy and Minerals (GEM) Thelon tectonic zone research activity.

GEM-2 supported research in the central Ttz (Figs. 1, 2) has extended earlier studies of the Ttz - Slave boundary on the west side of the orogen to the Ttz - Rae boundary zone on the east side of the orogen. New understanding of the architecture of the central Ttz (Fig. 2) has been defined on the basis of high-resolution aeromagnetic data (Kiss et al., 2014a, b; Coyle et al., 2016a, b) combined with geological relationships (Berman et al., 2018; Thompson et al., 1986), plutonic rock geochemistry (Whalen et al., 2018), Sm-Nd-O isotopic data (Berman et al., 2020), and U-Pb zircon crystallization ages from TIMS (van Breemen et al., 1987, Frith and van Breemen, 1990) and SHRIMP data (Davis et al., 2013; 2014; W.J. Davis, unpublished data). The present study provides additional age constraints from a laser ablation, multi-collector inductively coupled mass spectrometry study of Neoarchean plutonic rocks of the eastern Slave craton (Bathurst block) and adjacent Paleoproterozoic plutonic rocks of the Ttz. In addition, one archival sample from further north, near Queen Maud Gulf (Fig. 1), was studied in order to provide a potential constraint on the age of basement in that region.

REGIONAL GEOLOGY

The Ttz extends more than 500 km northward from the MacDonald fault to north of Queen Maud Gulf (Fig. 1). The Ttz comprises intensely deformed, steeply dipping, NNE-striking Paleoproterozoic metaplutonic rocks and subordinate supracrustal rocks flanked by reworked margins of the Slave (west side) and Rae (east side) cratons (Fig. 1). The core of the central Ttz comprises ca. 2.03 – 1.96 Ga intermediate to felsic granitoids whose whole rock geochemistry (Whalen et al., 2018) and O isotopic compositions (Berman et al., 2020) indicate genesis at a convergent plate tectonic setting. Two sequences of metasedimentary rocks are documented in the Ellice River domain (Fig. 2): ca. 2.09 – 2.02 Ga psammite, and ca. 1.95 – 1.9 Ga siltstone (Davis et al., 2020).

On the east flank of the Ttz, the Rae craton consists of Mesoarchean (ca. 3.2 – 2.9 Ga), upper amphibolite- to granulite-facies diorite to monzogranite (Davis et al., 2013, 2014; Berman et al., in prep.) of the Queen Maud block (QMb). Rocks correlative with the westernmost part of the QMb are identified in the Duggan Lake domain (DLd; Fig. 2), where granitoids are

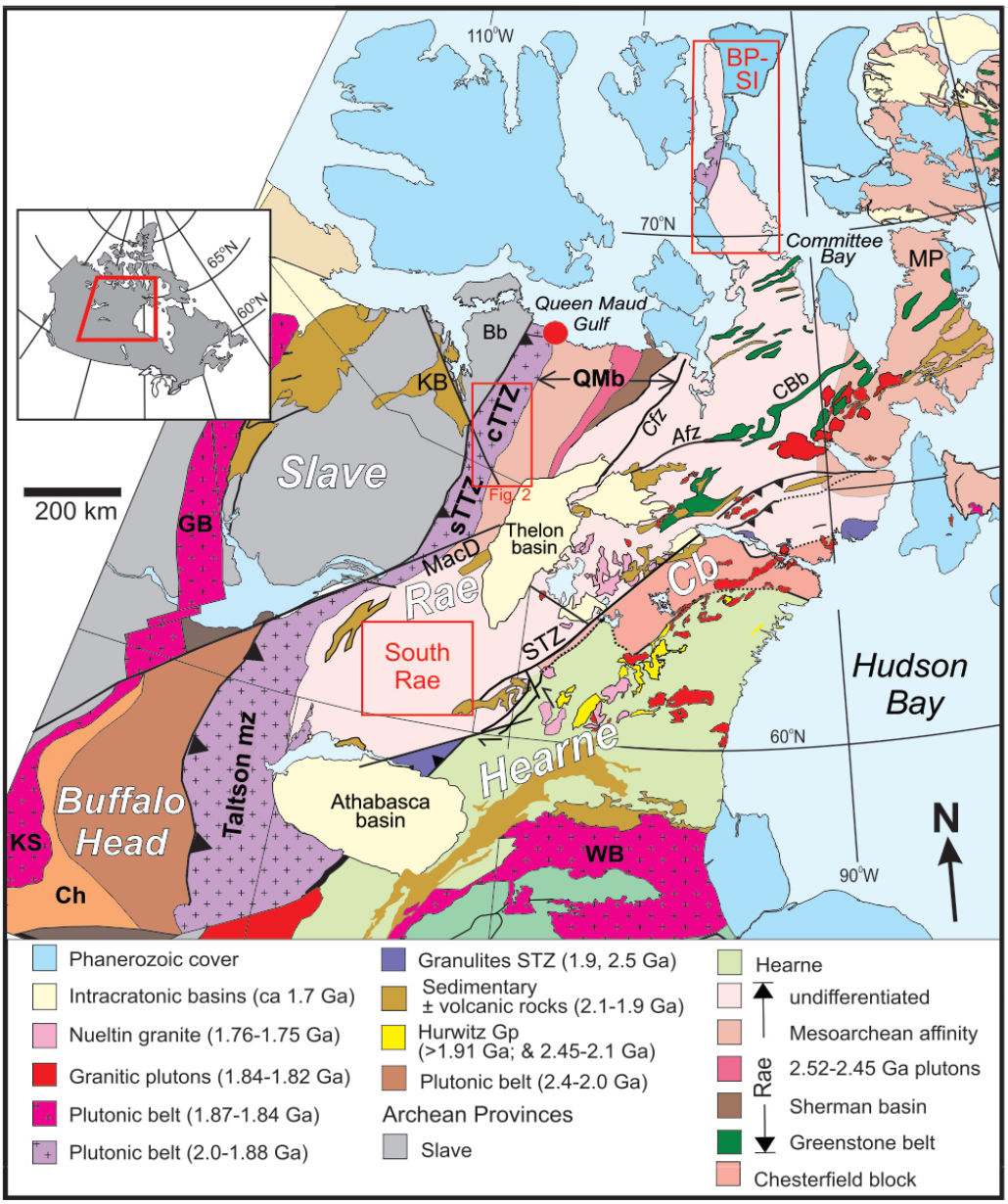

Figure 1. Geological map of northern Canada showing major tectono-magmatic elements and the location of three field-based GEM-2 activities (red boxes) focussed along western Rae craton, including the central Thelon tectonic zone project. Abbreviations: Afz=Amer fault zone; Bb = Bathurst block; BP-SI=Boothia Peninsula-Somerset Island; Cb=Chesterfield block; CBb=Committee Bay belt; Cfz=Chantrey fault zone; Ch = Chinchaga domain; GB = Great Bear; KB = Kilohigok basin; KS = Kitsuan magnetic high; MacD = MacDonald fault; MP=Melville Peninsula; mz=magmatic zone; QMb=Queen Maud block; Stz=Snowbird tectonic zone; sTTZ = southern Thelon tectonic zone; cTTZ = central Thelon Tectonic Zone; WB= Wathaman batholith. Location of sample 62-PB288 is shown by red circle just south of Queen Maud Gulf.

isotpically (U-Pb, Sm-Nd) indistinguishable from those further east (Berman et al., in preparation). The western boundary of the QMb (including the DLd) is marked by a >400 km-long domain of low magnetic response that comprises strongly foliated to mylonitic ca. 1.91 Ga peraluminous leucogranite with lesser garnet-sillimanite diatexite and garnet-free monzogranite (van Breemen et al., 1987; Berman et al., 2018, 2020).

On the west side of the central Ttz, the Bathurst block of the eastern Slave craton (Fig. 1) is divided here informally into the Tinney Hills and Overby Lake domains (Fig. 2). The THd is dominated by metapelitic rocks of the Yellowknife Supergroup which are intruded by ca. 2.6 Ga two-mica granitoid and tonalite (Culshaw and van Breemen, 1990) as well as undated granodioritic - monzogranitic granitoids (Frith, 1982; Thompson et al., 1986). Metamorphic grade increases eastward from lower- to upper-amphibolite facies, culminating in the OLd, where strongly foliated, migmatitic granitoid gneisses host thin zones dominated by fine- to medium-grained amphibolite with minimal exposure of metapelitic rocks (Thompson et al., 1986). Tonalitic to granodioritic plutonic rocks in the OLd are metaluminous and less potassic and magnesian than THd granitoids, which include peraluminous, two-mica granitoids (Whalen et al., 2018). Compared to THd granitoids, OLd granitoids have slightly more evolved Nd isotopic character (Berman et al., 2020).

The Ttz has been strongly deformed during multiple episodes of deformation interpreted to reflect NW-directed thrusting driven by convergence between the Slave and Rae cratons, followed by dextral transpression during indentation of the Slave craton (Hoffman, 1988; Culshaw, 1991; Ma, 2019). Five main metamorphic events are recognized in the study area (Davis et al., 2015; Mitchell et al., 2017; Berman et al., 2018): (1) ca. 2.58 Ga in the Tinney Hills domain, (2) ca. 2.4-2.35 Ga in the Duggan Lake domain and Queen Maud block, (3) ca. 2.0 Ga regional contact metamorphism associated with emplacement of Ttz plutonic belts, (4) 1.92-1.89 Ga upper amphibolite- to granulite-facies metamorphism (the most widespread event; Fig. 2), and (5) ca. 1.82 Ga lower amphibolite-facies metamorphism recognized in several locations across the central Ttz (Davis et al. 2014; Mitchell et al. 2017).

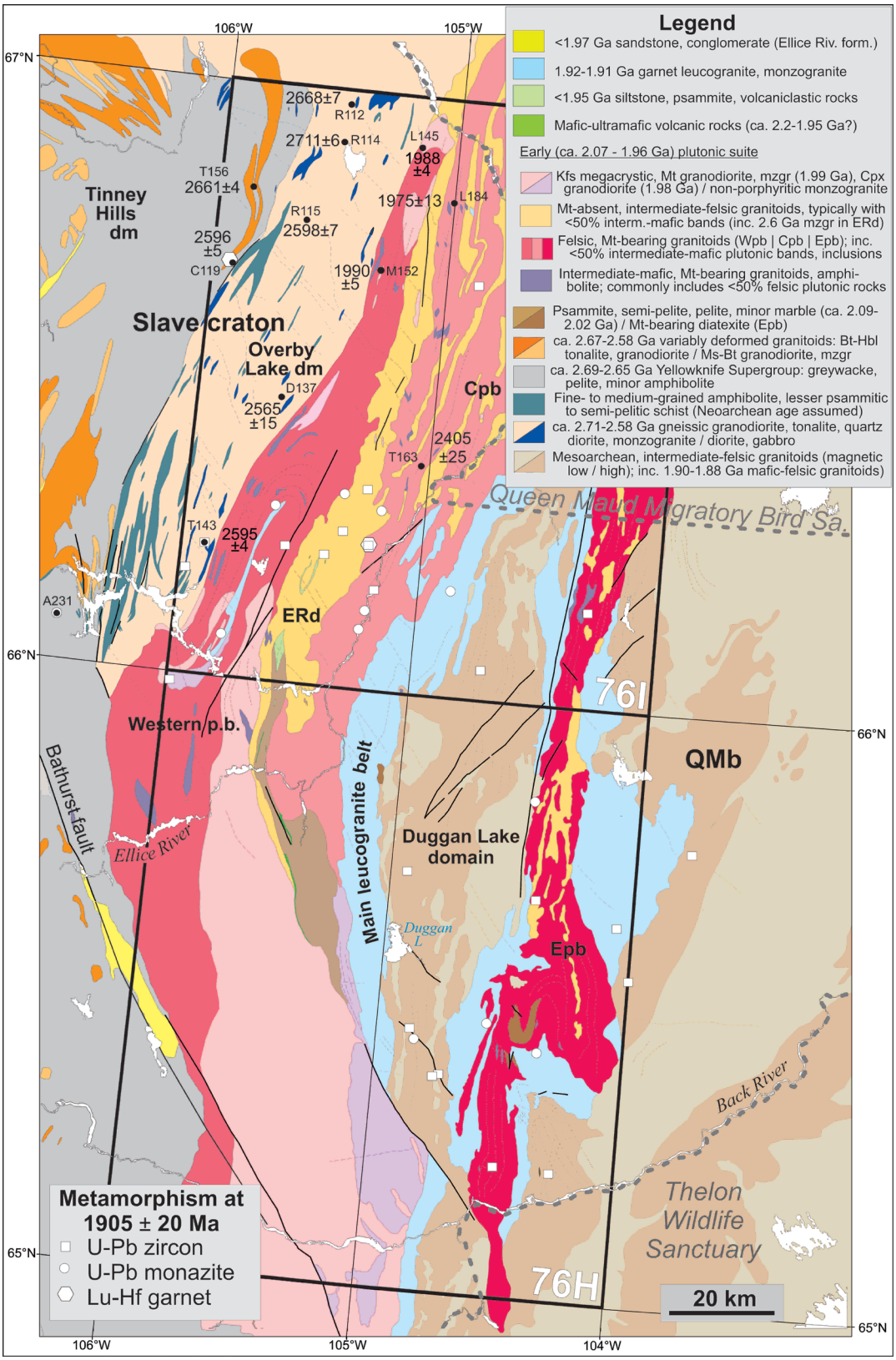

Figure 2. Simplified geologic map of the central Ttz (NTS map sheets 76H and 76I) showing crustal domains and location of samples. Abbreviations: dm = domain; p.b. = plutonic belt; QMb = Queen Maud block.

METHODS

Analytical data were collected from polished 30 micron-thick thin sections. Back-scattered SEM imaging was used to characterize zoning and core-rim relationships in analyzed zircon grains. U-Pb zircon data was collected using laser ablation multi collector inductively coupled mass spectrometry (LA-MC-ICPMS) at the Canadian Centre for Isotopic Microanalysis at the University of Alberta, Edmonton, Canada using procedures modified from Simonetti et al. (2005). The analytical setup consists of a New Wave UP-213 laser ablation system interfaced with a Nu plasma MC-ICPMS equipped with three ion counters and 12 Faraday cups. We operated the laser at 4 Hz with a beam diameter of 30 um which yielded a fluence of ~1-3 J/cm^2. Ablations were conducted in a He atmosphere at a flow rate of 1 L/min through the ablation cell. Output from the cell was joined to the output from a standard Nu plasma desolvating nebulizer (DSN-100). On peak gas + acid blanks (30s) were measured prior to a set of analyses. Data was collected statically consisting of 30 1s integrations. Before and after each set of analyses, zircon reference materials GJ1 (LH9415; Ashton et al., 1999; Jackson et al., 2004) and Plesovice (OG1; Stern et al, 2009; Sláma et al., 2008) were repeatedly analyzed, to monitor and correct for U-Pb fractionation, reproducibility, instrument drift, and to assess data quality. Mass bias for Pb isotopes was corrected by measuring $^{205}Tl/^{203}Tl$ from an aspirated Tl solution (NIST SRM 997) via the DSN-100 desolvating nebulizer using an exponential mass fractionation law and assuming a natural $^{205}Tl/^{203}Tl$ of 2.3871. All data were reduced offline using an Excel-based program. Unknowns were normalized to GJ1 (LH9415) as the primary reference and Plesovice (OG1) was treated as an unknown to assess data quality. The uncertainties reported are a quadratic combination of the internal measurement precision and the overall reproducibility of the standards during an analytical session. The long term 2σ reproducibility for the standards is estimated to be ~1% for $^{207}Pb/^{206}Pb$ and 2% for $^{206}Pb/^{238}U$. The data are not corrected for common Pb due to the difficulty in resolving transient contributions of ^{204}Hg present in the Ar gas from ^{204}Pb present in either the crystal and/or the acid + gas blank. Thus reported ^{204}Pb values are for informational purposes only, but can be useful for identifying and rejecting samples that have obviously large amounts of common Pb.

RESULTS

Isoplot v. 4.15 (Ludwig 2012) was used to generate concordia plots and calculate dates (Table 1) from analytical data presented in Appendix 1. The error ellipses on Concordia diagrams and in Table 1 and the text are reported at 95% confidence intervals. Results summarized below document derivation of age dates from the most concordant data; a discordancy cut-off of 2-3% was used, depending on both the quality and number of analyses collected.

Many of the samples discussed below show a range of age analyses outside of a single statistical population. In the absence of chemical correlations, and given the well documented, widespread ca. 1.9 Ga metamorphism that affected this region, this spread in ages is interpreted to reflect Pb loss or mixed analyses that incorporated metamorphic rims as well as igneous cores. Three methods are generally considered to derive the best estimate of the igneous crystallization age from such data. Constrained regression, with the lower intercept fixed at the time of high-grade metamorphism (1905 ± 20 Ma), yields an upper intercept that generally represents the maximum crystallization age; this assumes all analyses are affected to some extent by Pb loss or mixed age domains. Isoplot's Unmix function is useful for characterizing the distribution of age populations; this function yields a crystallization age from the assumed normal distribution of results around the maximum age mode. The preferred method applied here is to derive the crystallization age from the weighted mean of the oldest $^{207}Pb/^{206}Pb$ ages that from a coherent statistical population (e.g. MSWD < 2). This method implicitly assumes these analyses have been minimally affected by Pb loss or mixed age domains, and is supported by the observed correlation in most samples between age and the size of the zircon domain analysed. Small grains, commonly with distinct, unzoned, presumably metamorphic rims, generally yield younger results.

In the results presented below, data not included in determining a date are referred to either as "rejected", if rejected by Isoplot as statistical outliers, or as "excluded", if manually excluded on the basis of discordancy or to improve the coherency of a statistical population. Whole rock geochemistry and Sm-Nd isotopes are presented elsewhere (Whalen et al., 2018; Berman et al., 2020) for most of the samples discussed below.

Paleoproterozoic Thelon tectonic zone plutonic rocks:

16BLB-L145: coarse-grained, moderately foliated Hbl-Bt granodiorite (Western plutonic belt)

Analyzed zircon grains are commonly 50 x 100 microns in size, and most show concentric zoning diagnostic of igneous crystallization (Fig. 3A). Rare grains have distinct, metamict cores, with thick, concentrically zoned rims. Thirty-one analyses of 26 grains yield $^{207}Pb/^{206}Pb$ ages from ca. 2014 to 1930 Ma (Fig. 3A). Seven analyses have discordance greater than 3%. Excluding these, 24 analyses yield a weighted mean $^{207}Pb/^{206}Pb$ age of 1988 ± 4 Ma (MSWD = 0.8; 1930 Ma analysis rejected), which is interpreted as the crystallization age of this rock.

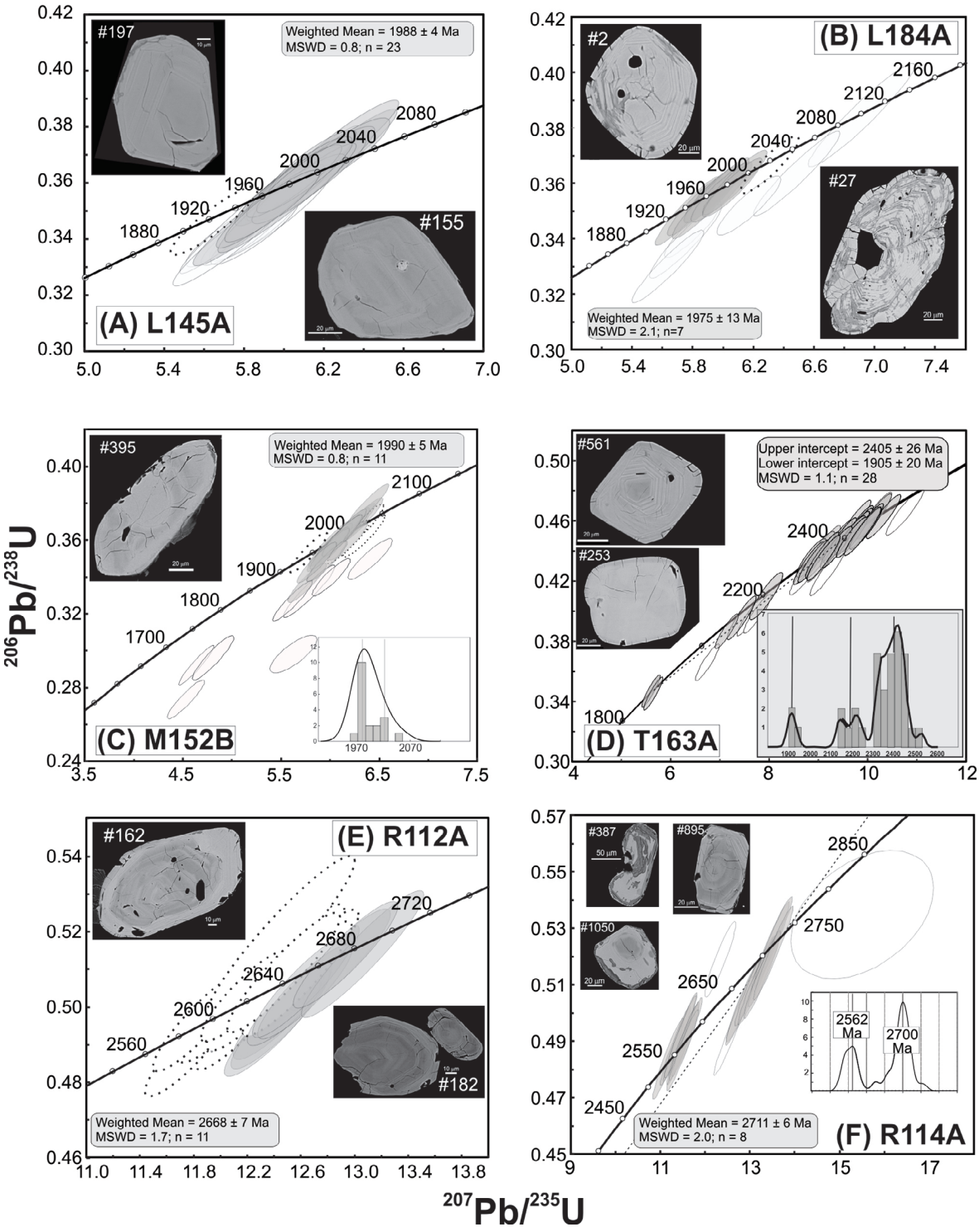

Figure 3. U-Pb Concordia plots for samples discussed in text. Shaded ellipses show data used to determine date; discordant data = solid, unfilled ellipses; rejected/excluded analyses = dotted, unfilled ellipses. Insets show representative back-scattered SEM images of analyzed zircon grains. Isoplot age distribution diagrams are shown for selected samples. See text for discussion.

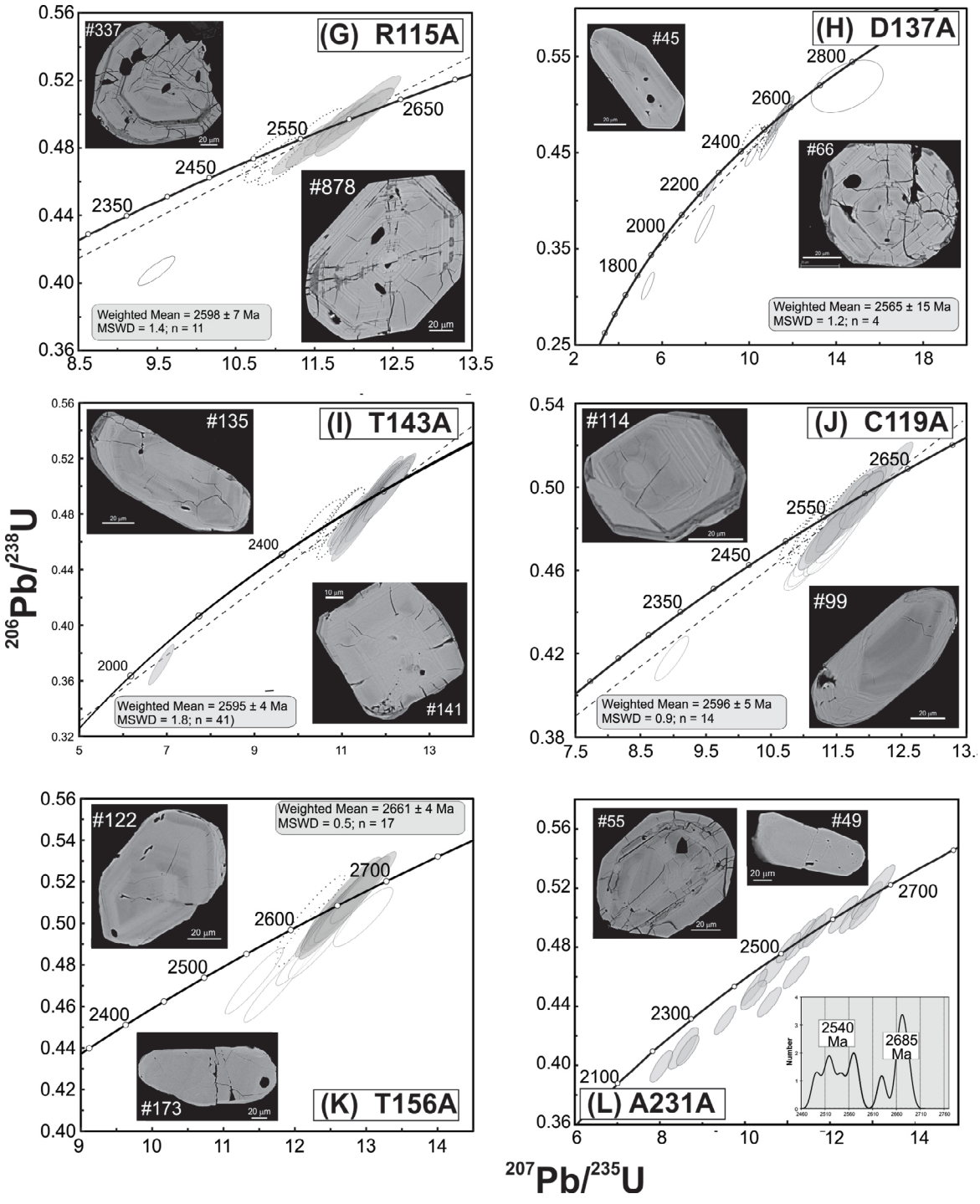

Figure 3 (continued). U-Pb Concordia plots for samples discussed in text.

Table 1: Summary of U-Pb zircon age determinations

Sample	Lithology	Domain	Age (Ma)	MSWD	POF	n	Age Details	Latitude	Longtitude
L145A	Granodiorite	Wpb	1988 ± 4	0.8	0.69	23	w.mean	66.92518	-105.1560
L184A	Granodiorite	Wpb	1975 ± 13	2.1	0.01	7	w.mean	66.82459	-105.0024
M152B	Monzogranite	Wpb	1990 ± 5	0.8	0.66	11	w.mean	66.70597	-105.2835
T163A	Quartz monzonite	Cpb	2405 ± 25	1.1	0.38	28	u.i.	66.38514	-105.0383
R112A	Tonalite	OL	2668± 7	1.7	0.08	11	w.mean	66.97827	-105.4820
R114A	Granodiorite	OL	2711 ± 6	2.0	0.05	8	w.mean	66.91328	-105.4898
R115A	Granodiorite	OL	2598 ± 7	1.4	0.16	11	w.mean	66.78025	-105.6216
D137A	Monzogranite	OL	2565 ± 15	1.2	0.29	4	w.mean	66.47638	-105.6399
T143A	Granodiorite	OL	2595 ± 4	1.8	0.001	41	w.mean	66.22019	-105.9008
C119A	Granodiorite	TH	2596 ± 5	0.9	0.6	14	w.mean	66.68777	-105.9172
T156A	Tonalite	TH	2661 ± 4	0.5	0.96	17	w.mean	66.82645	-105.8604
A231A	Metapelite	TH	(see text)	-	-	-	-	66.0743	-106.4774
PB288A	Tonalite	QMG	2615 ± 18	1.7	0.16	4	w.mean	67.92575	-103.6429

Sample prefixes = 16BLB-; except 62-PB288

Abbreviations: Cpb = central plutonic belt, OL = Overby Lake, TH = Tinney Hills, QMG = Queen Maud Gulf (see Fig. 1); Wpb = western plutonic belt

Age ± 2σ; n = number of analyses used in age determination

Age details: Concordia age; u.i. = upper intercept age with lower intercept fixed at 1905 ± 20 Ma; w.mean = weighted mean 207Pb/206Pb age

16BLB-L184: medium-grained, moderately foliated, Opx-Bt granodiorite (Western plutonic belt)

The scarcity of zircon greater than 40 microns in size in this sample limited analyses to eight grains. Most grains (e.g. #27, 132; Fig. 3B) display strong concentric zoning consistent with igneous crystallization. Eighteen analyses of the eight grains analyzed yield $^{207}Pb/^{206}Pb$ ages from ca. 2520 to 1947 Ma (Fig. 3B). Eight analyses have discordance greater than 3%. Of the remaining 10 analyses, which are less than 1% discordant, two are slightly older, ca. 2101 and 2024 Ma. The laser spots for these overlap cores and are interpreted as inherited; the 2024 Ma result is also a statistical outlier (i.e. rejected by Isoplot). The youngest (1947 Ma) analysis was obtained from a small zircon grain and overlaps a wide, presumably metamorphic rim. The remaining seven analyses yield a weighted mean $^{207}Pb/^{206}Pb$ age of 1975 ± 13 Ma age (MSWD = 2.1), which is interpreted as the crystallization age of this rock.

16BLB-M152B: coarse-grained, strongly foliated, Hbl-Bt monzogranite (Western plutonic belt)

Analyzed zircon grains vary from equant ~50 x 50 micron-wide, euhedral crystals (#141) to ~40 x 150 micron, rounded, partially to strongly embayed grains which commonly display cores with darker BSE response and patchy zoning (#123). Most of the 12 grains analyzed display concentric zoning diagnostic of igneous crystallization (eg. #141; Fig. 3C). Excluding the 14 age results that are >3% discordant, the remaining fifteen analyses yield $^{207}Pb/^{206}Pb$ ages from ca. 2027 to 1934 Ma (Fig. 3C). The distribution of these ages is bimodal, with peaks at 1990 ± 6 and 2027 ± 9 Ma (relative misfit = 0.78). Given the documented presence of 2030 – 2011 Ma plutonic rocks in the Wpb (Davis et al., 2014; Berman et al., 2018) and the large ca. 2020 Ma mode in Ellice River domain cycle 2 metasedimentary rocks, we attribute the older group of ages to inherited zircons; most of these analyses derive from the more elongate population of zircons with discernable cores (#123, 395; Fig. 3C). The younger group of twelve, < 2% discordant analyses yields a weighted mean $^{207}Pb/^{206}Pb$ age of 1990 ± 5 Ma (MSWD = 0.8; 1934 Ma datum rejected), which is taken as the crystallization age of this rock.

T163A: medium- to coarse-grained, strongly foliated Opx-Bt quartz monzonite (Central plutonic belt)

Abundant zircon occurs primarily as equant, ~40 - 80 micron-wide, generally unfractured grains with concentrically zoned cores surrounded by thin (< 10 microns), unzoned rims (Fig. 3D). One exception is grain #253 (Fig. 3D), a 70 micron-wide, unzoned crystal with several large fractures partly transecting it. Two analyses on this grain yield ca. 1.91 Ga, nearly concordant results, interpreted as the time of metamorphism. As a group, the 28 analyses obtained for this sample, excluding the dates that are > 2% discordant, can be fitted within error to a single discordia chord having intercepts at 1969 ± 67 Ma and 2408 ± 30 Ma (MSWD = 0.96). Assuming a lower intercept of 1905 ± 20 Ma, the well documented time of high-grade metamorphism across the central Ttz (Mitchell et al., 2017), yields an upper intercept $^{207}Pb/^{206}Pb$ age of 2405 ± 25 Ma (MSWD = 1.1), which is taken as the time of igneous crystallization.

The interpreted age is very similar to a 2408 ± 4 Ma tonalite in the Mesoarchean Duggan Lake domain (i.e. western QMb). However the Duggan Lake domain tonalite is isotopically more evolved (ε_{Nd} (2408 Ma) = -4.9) than sample T163A (ε_{Nd} (2405 Ma) = 2.7). In the absence of data for additional samples, as well as a petrologic model for ca. 2.4 Ga plutonism, the significance of this difference is unclear.

Neoarchean plutonic rocks of the Overby Lake domain:

16BLB-R112A: medium- to coarse-grained, strongly foliated Bt tonalite

Analyzed zircon grains are equant to prismatic and between 70 – 200 microns in length. Fractures in many grains are generally limited to short, discontinuous segments in cores which are commonly surrounded by unfractured rims. All grains show concentric zoning indicative of igneous crystallization (Fig. 3E). Seventeen <3 % discordant analyses of 9 grains yield a skewed $^{207}Pb/^{206}Pb$ age distribution from ca. 2691 to 2588 Ma (Fig. 3E). Mixture modelling (Sambridge & Compston, 1994) yields peaks at 2666 ± 6 Ma and 2617 ± 6 Ma with a fairly high misfit (0.59). Age results correlate well with the size of unfractured cores, supporting the interpretation that younger ages reflect Pb loss or mixed analyses. Accordingly, the crystallization age is derived from the weighted mean of the oldest statistically coherent group of analyses (2668 ± 7 Ma; MSWD = 1.7; n = 11). A very similar, but less precise, age results from the upper intercept (2667 ± 28 Ma; MSWD = 2.8) with the lower intercept constrained to 1905 ± 20 Ma.

16BLB-R114A: fine-grained, moderately foliated Bt granodiorite

Most zircon occurs as equant ~60 x 60 micron grains to 50 x 100 micron prisms. Smaller grains show oscillatory zoning (#895; Fig. 3F) suggesting igneous crystallization. Several larger grains have uniform interiors with no or very subtle internal zonation (#387; Fig. 3F). One grain has a zoned core, partially surrounded by an unzoned rim (#1050; Fig. 3F). Thirty analyses, ranging from ca. 2906 to 2531 Ma (Fig. 3F), were obtained from 14 grains. All but 4 analyses are less than 3% discordant. Excluding these 4 analyses, mixture modelling shows a strong grouping of $^{207}Pb/^{206}Pb$ ages at 2700 ± 3 Ma and 2560 ± 4 Ma, with a relative misfit of 0.13 (Fig. 3F, inset). As the older ages correlate with grains displaying oscillatory zonation, a ca. 2700 Ma crystallization age is indicated. The best estimate of this age is taken as the weighted mean $^{207}Pb/^{206}Pb$ age of the oldest nine analyses, 2711 ± 6 (MSWD = 2.0; 2754 Ma analysis rejected). The significance of the younger (ca. 2560 Ma) age population is unclear. The absence of evidence for metamorphism at this time suggests it reflects a younger phase of magmatism similar to the ca. 2560 Ma age of monzogranite sample D137A (Fig. 2; Table 1).

16BLB-R115A: fine to medium-grained, moderately to strongly deformed, Hbl-Bt granodiorite

Analyzed zircon grains are equant to prismatic grains, more than 50 microns in diameter and up to 300 microns in length. Except for unzoned small cores which were not analyzed, most grains are concentrically zoned core to rim (Fig. 3G), consistent with igneous crystallization. With the exception of two analysis that are > 3% discordant (Fig. 3G), the remaining sixteeen analyses on 8 grains yield $^{207}Pb/^{206}Pb$ ages ranging from ca. 2613 to 2511 Ma (Fig. 3G), with a skewed distribution showing peaks at ca. 2534 and 2596 Ma. Regression of these analyses yields an upper intercept $^{207}Pb/^{206}Pb$ age of 2602 ± 36 Ma and lower intercept of 2137 ± 370 Ma

(MSWD = 1.6). A maximum crystallization age is taken as the upper intercept $^{207}Pb/^{206}Pb$ age of 2594 ± 19 Ma (MSWD = 1.5) that results from constraining the lower intercept to 1905 ± 20 Ma. The weighted mean $^{207}Pb/^{206}Pb$ age of the oldest 11 analyses yields 2598 ± 7 Ma (MSWD = 1.4), which is taken as the best estimate of the crystallization age of this rock.

16BLB-D137A: coarse-grained, weakly foliated Bt monzogranite

Zircon in this sample are generally equant and less than 60 microns in size. Variable degrees of fracturing limited the number of grains and spots that could be analyzed. All grains show concentric zoning indicative of igneous crystallization (Fig. 3H). Nine of the eighteen analyses on 8 grains are >3% discordant and are not included. The nine more concordant analyses yield a skewed $^{207}Pb/^{206}Pb$ age distribution from ca. 2575 to 2272 Ma Ma (Fig. 3H) with a mode at 2565 ± 9 Ma (fraction = 0.50). Fixing a lower intercept of 1905 ± 20 Ma yields an imprecise upper intercept age (2563 ± 34 Ma; MSWD = 1.6). The best estimate of the crystallization age is taken as the weighted mean $^{207}Pb/^{206}Pb$ age of the oldest 4 analyses: 2565 ± 15 Ma (MSWD = 1.2).

16BLB-T143A: medium-grained, weakly foliated Bt granodiorite

Analyzed zircon grains are commonly equant to prismatic and greater than 50 microns in shortest dimension. Many grains show concentric zoning consistent with igneous crystallization (e.g. #135, 141; Fig. 3I). Excluding seven analyses that are > 3% discordant, 46 analyses of 33 grains yield an array of $^{207}Pb/^{206}Pb$ ages from ca. 2615 to 2478 Ma; Fig. 3I), with a strong mode at ca. 2595 Ma and minor peak at ca. 2520 Ma. Fixing a lower intercept of 1905 ± 20 Ma yields a 2607 ± 16 Ma upper intercept, which is considered the maximum crystallization age. The same analyses yield a weighted mean $^{207}Pb/^{206}Pb$ age of 2595 ± 4 Ma (MSWD = 1.8; five youngest analyses rejected), which is interpreted as the best estimate of the crystallization age.

Neoarchean plutonic rocks of the Tinney Hills domain:

16BLB-C119A: fine to medium-grained, moderately foliated Hbl-Bt granodiorite

Analyzed zircon grains are most commonly, unfractured, prismatic grains ~50 x 100 microns in size. Some grains are concentrically zoned from core to rim (Fig. 3J), whereas others have cores with little or wide diffuse zones. Fifty-three analyses yield $^{207}Pb/^{206}Pb$ ages from ca. 2614 to 2529 Ma (Fig. 3J), not including a 2412 Ma, 7% discordant analysis. The 23 most concordant analyses (<3% discordant) have a skewed distribution with peaks at ca. 2592 and 2549 Ma. Constraining the lower intercept to 1905 ± 20 Ma gives an upper intercept of 2618 ± 17 Ma; MSWD = 1.5), which is interpreted as the maximum age of this rock. A weighted mean

$^{207}Pb/^{206}Pb$ age of 2596 ± 5 Ma (MSWD = 0.9), derived from the oldest 14 analyses, is taken as the best estimate of the crystallization age.

16BLB-T156A: medium- to coarse-grained, moderately foliated Bt tonalite

Most analyzed zircon grains are fairly equant, subhedral, often broken grains between 50 – 80 microns in size. Almost all show wide concentric zoning consistent with igneous crystallization (Fig. 3K). One larger grain had less obvious zoning, but returned a similar age to other zoned grains. Only one grain had a distinct core, which was not analysed. Not including 17 more than 3% discordant analyses, 17 analyses yield $^{207}Pb/^{206}Pb$ ages from ca. 2669 to 2649 Ma (Fig. 3K), whereas two analyses of grain 192 are younger (ca. 2612, 2634 Ma). Excluding grain 192, the most concordant 17 analyses yield a weighted mean $^{207}Pb/^{206}Pb$ age of 2661 ± 4 Ma (MSWD = 0.5), which is interpreted as the crystallization age. Assuming a lower intercept of 1905 ± 20 Ma for the same analyses results in a slightly older upper intercept age of 2673 ± 20 Ma (MSWD = 0.52).

84TZ-A231A: Gt-St-Sil-Bt metapelite

Detrital zircons were analyzed in this metapelite in order to provide some constraints on its source region, although it should be noted that rigorous treatment would require analyses of far more grains (~100; Vermeesch, 2004) than found in this sample. Analyzed zircon grains comprise two textural groups that correlate with age. One group of zircon grains has concentrically zoned cores 20-40 microns in diameter, with unzoned rims up to 20 microns wide (e.g. #55; Fig. 3L). The other group has larger, unzoned grains up to 100 microns in longest dimension (e.g. #49; Fig. 3L). Of nineteen analyses, nine are less discordant than ±3%; these yield $^{207}Pb/^{206}Pb$ ages from ca. 2685 to 2514 Ma (Fig. 3L). The probability distribution has a roughly bimodal distribution with major peaks at ca. 2670 and 2540 Ma. The younger ages derive from the second group of unzoned grains, suggesting they represent metamorphic zircon.

In the eastern Slave craton, ca. 2.68 – 2.6 Ga plutonism is documented in several greenstone belts (e.g. van Breemen et al., 1992) as well as in the THd samples of this study. Monazite and titanite dating also reveals a ca. 2.5 Ga metamorphism in this region (Mitchell et al., 2017). The distribution of ages determined for sample A231 is thus consistent with a detrital population derived from a local Slave craton source, and contrasts markedly with sedimentary sequences in the Ellice River domain which are dominated by ca. 2.3 and 2.19 Ga detrital zircon peaks (Davis et al., in preparation).

Thelon tectonic zone – eastern basement

62-PB288A: coarse-grained, weakly to moderately foliated Bt tonalite (archival sample from near the Queen Maud Gulf; Fig. 1)

Only seven zircon grains were analyzed in this sample due to their scarcity and small size. Analyzed grains are well faceted, unfractured grains larger than 40 microns in diameter and up to 80 microns long. All grains have concentrically zoned cores surrounded by unzoned rims up to 10 microns in width (Fig. 4). Of the twelve analyses from these grains, seven are less than 3% discordant. The probability distribution forms peaks at ca. ca. 2615 Ma and 2546 Ma (relative misfit = 0.4). Assuming a lower intercept of 1905 ± 20 Ma yields an imprecise upper intercept age of 2603 ± 55 Ma (MSWD = 3.4). The best estimate of the crystallization age of this rock is taken as the weighted mean $^{207}Pb/^{206}Pb$ age of the oldest four analyses (2615 ± 18 Ma; MSWD = 1.7). The Nd model age of this sample is 2.87 Ga (Berman et al., 2020).

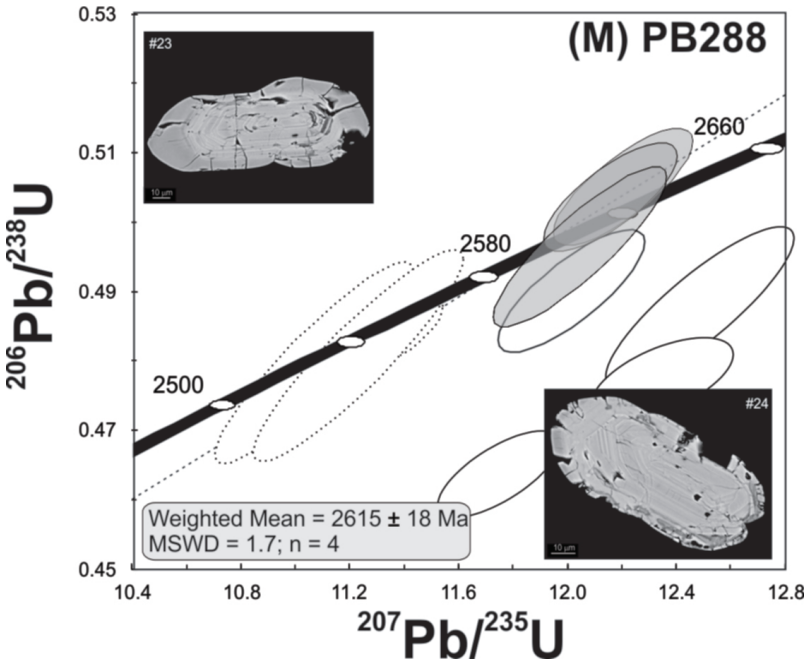

Figure 4. U-Pb Concordia plot for sample PB288. Insets show representative zircon Grains See Figure 3 caption for explanation of line and fill types.

HIGHLIGHTS

Twelve U-Pb zircon dates have been determined for plutonic rocks of the eastern Slave craton and adjacent Thelon tectonic zone. The most significant findings are:

- Both the THd and OLd host ca. 2.6 Ga plutonic rocks, as have been documented across the Slave craton (e.g. van Breemen et al., 1992; Villeneuve et al., 1997).
- 2.661 ± 0.004 Ga tonalite (sample T156A) dated in the THd is consistent with the oldest plutonic ages (2.686 – 2.679 Ga) documented in greenstone belts of the eastern Slave craton (van Breemen et al., 1992).
- The 2.711 ± 0.006 Ga age of granodiorite in the OLd (sample R114A) is within error of the SHRIMP U-Pb zircon age of 2.712 Ga monzogranite further east in this domain (Berman et al., 2020); these ages are similar to the oldest volcanic ages in the Yellowknife Supergroup, but document older plutonic rock ages in the OLd than recognized in Yellowknife Supergroup greenstone belts elsewhere in the Slave craton.
- 2.615 ± 0.018 Ga tonalite in the northern Ttz (sample PB288) indicates a crustal component other than Mesoarchean rocks of the QMb and ca. 2.03 – 1.90 Ga Ttz plutonic rocks.
- 2.405 ± 0.025 Ga monzogranite in the Central plutonic belt (sample T163A) is indistinguishable in age from a tonalite intruding the western QMb, consistent with potential linkage between the QMb and basement to the Central plutonic belt.

ACKNOWLEDGMENTS

The authors thank Tim Chadwick, Dustin Likane, Léo Nadeau and Mary Sanborn-Barrie for their field observations and assistance in sample collection, Pat Hunt for SEM assistance, and Bruce Kjarsgaard for a constructive review of a first draft of this contribution.

REFERENCES

Ashton, K.E., Heaman, L.E., Lewry, J.F, Hartlaub, R.P., and Shi, R., (1999) Age and origin of the Jan Lake Complex: a glimpse at the buried Archean craton of the Trans-Hudson Orogen, Canadian Journal of Earth Science, 36, 185-208.

Berman, R.G., Taylor, B., Davis, W.J., and Whalen, J.B. (2020) The Thelon Tectonic Zone: new insights into its crustal architecture and tectonic setting from Sm-Nd and O isotopes Geological Survey of Canada Bulletin (in press).

Berman, R.G., Davis, W.J., Sanborn-Barrie, M., Percival, J.A., Whalen, J. and Nadeau, L., in preparation. Isotopic constraints on the architecture and evolution of the northwestern Rae craton, Canada.

Berman, R.G., Davis, W.J., Sanborn-Barrie, M., Whalen, J.B., Taylor, B., McMartin, I., McCurdy, M.W., Mitchell, R., Ma, S., Coyle, M., Roberts, B. and Craven, J., 2018. Report of 2017 Activities: Chantrey-Thelon activity, Thelon tectonic zone project. GSC Open File 8372, 19p., doi:10.4095/306622.

Camacho, A., Berman, R.G., and Sanborn-Barrie, M. (2019) 40Ar/39Ar hornblende and biotite cooling ages for meta-plutonic rocks of the central Thelon tectonic zone, Nunavut. GSC Open File, 8625, 77p.

Chacko, T., De, S.K., Creaser, R.A., and Muehlenbachs, K., 2000. Tectonic setting of the Taltson magmatic zone at 1.9-2.0 Ga: A granitoid-based perspective; Canadian Journal of Earth Sciences, v. 37, p. 1597-1609.

Coyle, M., 2017a. Residual total magnetic field, aeromagnetic survey of the Overby-Duggan area, part of NTS 076-I south, Nunavut; GSC Open File, v. 8281, p. 1 sheet.

Coyle, M., 2017b. Residual total magnetic field, aeromagnetic survey of the Overby-Duggan area, part of NTS 076-I north, Nunavut; GSC Open File, v. 8282, p. 1 sheet.

Culshaw, N., 1991. Post-collisional oblique convergence along the Thelon tectonic zone, north of the Bathurst Fault, NWT, Canada; Journal of Structural Geology, v. 13, p. 501-516.

Culshaw, N.G. and van Breemen, O., 1990. A zoned low P-high T complex at the level of anatexis; structural and plutonic patterns in metasediments of the Archean Yellowknife Supergroup, near Bathurst Inlet, N.W.T., Canada. Precambrian Research 48, 1-20.

Davis, W., Berman, R.G., and MacKinnon, A., 2013. U-Pb Geochronology of Archival Rock Samples from the Queen Maud Block, Thelon Tectonic Zone and Rae Province, Kitikmeot Region, Nunavut, Canada; Geological Survey of Canada, Open File, v. 7409, p. 42p, doi:10.4095/292663.

Davis, W.J., Berman, R.G., and Nadeau, L. (2015) Mapping regional metamorphic events in poly-metamorphosed plutonic domains using recrystallized zircon; an example from the Paleoproterozoic Thelon tectonic zone and adjacent Queen Maud Block, northwestern Canada. V.M. Goldschmidt Conference - Program and Abstracts, 25, 675.

Davis, W.J., Berman, R.G., Nadeau, L., and Percival, J.A., 2014. U-Pb Zircon Geochronology of a Transect Across the Thelon Tectonic Zone, Queen Maud Region, and Adjacent Rae Craton, Kitikmeot Region, Nunavut, Canada. Geological Survey of Canada, Open File 7652, 38 pp doi:10.4095/295177

Davis, W., Sanborn-Barrie, M., Berman, R.G., and Pehrsson, S. (2020) Timing, provenance and tectonic significance of Paleoproterozoic supracrustal sequences in the central Thelon tectonic zone. Precambrian Research (submitted February, 2020).

Frith, R.A., 1982. Geology, Beechey Lake-Duggan Lake, District of Mackenzie; Geological Survey of Canada, Open File, v. 851 (1:125,000).

Frith, R.A., and van Breemen, O., 1990. U-Pb zircon age from the Himag plutonic suite, Thelon Tectonic Zone, Churchill Structural Province, Northwest Territories; Geological Survey of Canada, Paper, v. 89-2, p. 49-54.

Gibb, R.A. and Thomas, M.D., 1977. The Thelon Front; a cryptic suture in the Canadian Shield? Tectonophysics 38, 211-222.

Hoffman, P.F., 1988. United plates of America, the birth of a craton: Early Proterozoic assembly and growth of Laurentia; Annual Reviews of Earth and Planetary Science, v. 16, p. 543–603.

Jackson, S.E., Pearson, N.J., Griffin, W.L., Belousova, E.A. (2004), The application of laser ablation-inductively coupled plasma-mass spectrometry to in situ U–Pb zircon geochronology, Chemical Geology, 211, 47-69.

Kiss, F., 2014a. Residual total magnetic field, aeromagnetic survey of the Duggan Lake area, part of NTS 76-H/N, Nunavut. gscof 7521, doi:10.4095/293654.

Kiss, F., 2014b. Residual total magnetic field, aeromagnetic survey of the Duggan Lake area, part of NTS 76-I/S, Nunavut. gscof 7523, doi:10.4095/293656.

Ludwig, K.R., 1998, On the treatment of concordant uranium-lead ages: Geochimica et Cosmochimica Acta 62, 665-676.

Ludwig, K.R., 2012. User's manual for Isoplot 4.15. A geochronological Toolkit for Microsoft Excel. Berkeley Geochronology Center, Special Publication No. 5, Berkeley, California

Ma, S., Kellett, D.A., Godin, L., and Jercinovic, M.J. (2019) Localisation of the brittle Bathurst fault on pre-existing fabrics: A case for structural inheritance in the northeastern Slave craton, western Nunavut, Canada. Canadian Journal of Earth Sciences, in press.

Mitchell, R.K., Berman, R.G., Davis, W.J., and Carr, S., 2017. Paleoproterozoic Metamorphism of the Thelon Tectonic Zone and margins of the Slave and Rae Archean cratons - insights into the nature and timing of the Slave-Rae Collision; Geol. Ass. Can. Prog. Abst., v. 40, p. 265.

Sambridge, M.S. and Compston, W., 1994. Mixture modelling of multi-component data sets with application to ion-probe zircon ages. Earth and Planetary Science Letters, 128, 373-390.

Schultz, M.E.J., Chacko, T., Heaman, L.M., Sandeman, H.A., Simonetti, A., and Creaser, R.A., 2007. Queen Maud block: A newly recognized Paleoproterozoic (2.4-2.5 Ga) terrane in northwest Laurentia; Geology, v. 35, p. 707-710.

Sláma, Jiří , Košler, Jan, Condon, Daniel J., Crowley, James L., Gerdes, Axel, Hanchar, John M., Horstwood, Matthew S.A., Morris, George A., Nasdala, Lutz, Norberg, Nicholas, Schaltegger, Urs, Schoene, Blair, Tubrett, Michael N., Whitehouse, Martin J. (2008) Plešovice zircon — A new natural reference material for U–Pb and Hf isotopic microanalysis, Chemical Geology, 249, 1-35.

Soderlund and Johansson (2002) A simple way to extract baddeleyite (ZrO2), Geochemistry, Geophysics, Geosystems, https://doi.org/10.1029/2001GC000212

Simonetti A. Heaman, L.M., Hartlaub, R.P., Creaser, R.A., MacHattiea, T.G., and Bohmb, C. (2005) U–Pb zircon dating by laser ablation-MC-ICP-MS using a new multiple ion counting Faraday collector array, J. Anal. At. Spectrom., 20, 677-686.

Stern, Richard A., Bodorkos, S., Kamo, S. L., Hickman, A. H., and Corfu, F.(2009) Measurement of SIMS Instrumental Mass Fractionation of Pb Isotopes During Steiger R.H. and Jäger E., 1977. Subcommission on geochronology: convention on the use of decay constants in geo- and cosmochronology. Earth Planet. Sci. Lett. 36, 359-362.

Thompson, P., 1986. Geology, Tinney Hills-Overby Lake (West Half), District of Mackenzie, Northwest Territories; Geological Survey of Canada, Open File 1316 (1:125,000).

Thompson, P.H., 1989. An empirical model for metamorphic evolution of the Archaean Slave Province and adjacent Thelon tectonic zone, north-western Canadian Shield; *in* Daly, J.S., Cliff, R.A., and Yardley, B.W.D. eds.), Evolution of metamorphic belts, Geological Society Special Publication, v. 43, p. 245-263.

van Breemen, O., Davis, W.J., and King, J.E. (1992) Temporal distribution of granitoid plutonic rocks in the Archean Slave Province, northwest Canadian Shield. Canadian Journal of Earth Sciences, 29, 2168-2199.

Van Breemen, O., Thompson, P.H., Hunt, P.A., and Culshaw, N., 1987. U - Pb zircon and monazite geochronology from the northern Thelon Tectonic Zone, District of Mackenzie; Geological Survey of Canada Paper, v. 87-2, p. 81-93.

Vermeesch, P., 2004. How many grains are needed for a provenance study? Earth and Planetary Science Letters, 224, 441–451.

Whalen, J. B., R. G. Berman, W. J. Davis, M. Sanborn-Barrie and L. Nadeau (2018). Bedrock geochemistry of the central Thelon tectonic zone. Geol. Surv. Canada Open File 8234: 27p.